



Fermi National Accelerator Laboratory

FERMILAB-Pub-91/99

Prospects for Using Photosensitive Dopants to Improve the e/π Ratio of Liquid Argon Calorimeters*

D. F. Anderson and N. A. Amos
Fermi National Accelerator Laboratory
P.O. Box 500
Batavia, Illinois 60510

June 1991

* Submitted to *Nuclear Instruments and Methods A*.



Prospects for Using Photosensitive Dopants to Improve the e/π Ratio of Liquid Argon Calorimeters

D.F. Anderson and N.A. Amos
Particle Detector Group
Fermi National Accelerator Laboratory
Batavia IL 60510 U.S.A.

(Submitted to Nuclear Instruments and Methods A)

Abstract

There is evidence that shows that heavily ionizing interactions contribute to the signal from hadrons in liquid argon calorimeters, and that saturation effects play an important role in the e/π ratio. Measurements and calculations are presented which indicate a substantial improvement can be made to the e/π ratio by the addition of a few ppm of photosensitive dopants.

1. Introduction

Saturation effects in liquid argon, LAr, can dominate the charge collected from the interactions of heavily ionizing particles such as alpha particles or heavy ions. In such cases, most of the charge is lost through recombination. With increased recombination comes a proportional increase in the scintillation yield[1]. The problem of saturation has been addressed in two ways: 1) the scintillation light is detected with a photomultiplier, the signal is weighted, and then added to the direct charge signal[2]; 2) photosensitive dopants are added directly to the LAr so that the scintillation light is converted back into detectable charge[3-8]. In the second technique the photons are converted some distance from the region of high charge density and thus the resulting charge is less susceptible to recombination.

Recently, a measurement and a calculation have shown that saturation effects are important to the relative response of a LAr calorimeter to electromagnetic and hadronic showers. This is often called the e/π ratio. The measurement was made by the HELIOS experiment at CERN with their U/LAr calorimeter[9]. They added a small amount of methane to the calorimeter to increase the electron drift velocity and saw a significant increase in the e/π ratio associated with increased saturation effects. Figure 1 shows the e/π ratio for the HELIOS calorimeter as a function of particle energy for pure LAr. We have added a logarithmic fit to these data to guide the eye. There is also a single measurement made with the addition of 0.35% methane at an energy of 100 GeV. The e/π ratio increased from about 1.09 at that energy to about 1.15 with the addition of methane. Ideally, e/π would equal 1. The increase in the e/π ratio shows that there is a substantial amount of heavily ionizing interactions in the hadron showers which are suppressed by the addition of the methane (see section 2.1).

A simulation has been made by J. Brau[10] of a U/LAr calorimeter where it is estimated that for a 5 GeV pion, of the 402 MeV deposited in the LAr, only 308 MeV is detected due to saturation effects. Of the 94 MeV that is lost, 72 MeV is from neutron interactions. It is important to detect these neutrons since they are correlated with the nuclear binding energy losses. In the simulation, it was shown that if the saturation effects could be removed from the LAr the e/π ratio would decrease from a quoted value of 1.2 to 0.9. The calorimeter would then be over-compensating.

The information presented above argues strongly for the addition of a photosensitive dopant to reduce the saturation effects in LAr with an improvement in the e/π ratio. This should be true for calorimeters using lead as well as uranium as the converter.

2. Dopants for LAr

There have been two type of dopants used in LAr: dopants such as methane to increase the drift velocity of the electrons, and photosensitive dopants to reduce the saturation effects. Both types change the saturation effects of the LAr. One way to parameterize the effect is to assume that the relationship between the signal and the dE/dx of the energy deposit obeys Birk's Law for scintillators (rewritten for collected charge)[11]:

$$\frac{dQ}{dx} = \frac{c \, dE/dx}{1 + k_B \, dE/dx} \quad (1)$$

Here Q is the amount of charge collected, c is a proportionality constant and k_B is Birk's constant (in units of $\text{g MeV}^{-1} \text{cm}^{-2}$). As k_B increases in value the saturation effects increase.

It should be emphasized that the determinations of k_B made below are made from only two values of dE/dx (minimum ionizing electrons and 5.5 MeV alpha particles from an ^{241}Am radiation source). There was not a third value of dE/dx used as a verification that pure or doped LAr really does obey Birk's Law. Because of this, the values of k_B quoted are to give the magnitude of the effects only.

2.1 Methane

Methane and ethane have been added in small amount ($\leq 0.5\%$) to LAr to "cool" the excess electrons. This increases the electron mobility and decreases the diffusion. Improvements of greater than a factor of two in mobility have been achieved in this way[12].

It is sometimes mistakenly assumed that the the addition of methane will decrease the the e/π ratio of a LAr calorimeter by the addition of hydrogen to the readout. The methane increases the saturation effects by greatly reducing the thermalization length of the electrons thus increasing the probability of recombination. Because of this, the recoil protons contribute little to the signal. Above a concentration of about 5% methane, the only signal from an alpha particle is from the few delta rays escaping the region of high charge density[11]. There is also a substantial loss in signal from minimum ionizing particles. For an electric field of 2 kV/mm, k_B is about $4.9 \times 10^{-3} \text{ g MeV}^{-1} \text{cm}^{-2}$ for pure LAr. With the addition of 0.35% methane, we have measured k_B be about $1.8 \times 10^{-2} \text{ g MeV}^{-1} \text{cm}^{-2}$ for the same electric field. For an electric field of 2.5 kV/mm the addition of 0.35% methane increases k_B from $4.0 \times 10^{-3} \text{ g MeV}^{-1} \text{cm}^{-2}$ to about $1.5 \times 10^{-2} \text{ g MeV}^{-1} \text{cm}^{-2}$. Thus the

addition of this small amount of methane increases kB by factors of about 3.7 for electric fields of 2 kV/mm and 2.5 kV/mm.

2.2 Photosensitive Dopants

Photosensitive dopants decrease the saturation effects by converting the scintillation light from recombination into photoionization some distance away from the heavy ionization. Photosensitive dopants increase the charge collected from alpha particles by a factor of two at 2 kV/mm while the signal from beta particles is only increased by about 13 % [4]. This implies a substantial reduction in kB.

One might hope that a sufficient amount of photosensitive dopant could be added to the LAr so that there would be both the reduction in saturation and provide the hydrogen to thermalize the neutrons in the shower. Unfortunately, all known photosensitive dopants have solubilities in the 10's of ppm level or less. Another suggestion is that a mixture of methane and a photosensitive dopant be added; the methane to provide the hydrogen (H_2 has negligible solubility in LAr [13]) and the photosensitive dopant to reduce kB. We have found that the addition of even a small amount of methane to LAr containing a photosensitive dopant negates all effects of the photosensitive dopant. This is due to the methane competing with the photosensitive dopant for the scintillation light. The methane is always added in much higher concentrations than the ppm levels of the photosensitive dopants.

3. Experimental Setup

A glass dewar with a 10 cm inside diameter was used for the measurements. The silvering was removed from a 1 cm vertical strip so that the liquid level could be accurately determined as well as to look for undissolved dopant which can be seen as small colloids in a bright light.

The argon gas entered the dewar at the bottom through a stainless steel frit in order to produce turbulence and mixing in the liquid. It was found that dopants in LAr mix very slowly unless vigorously agitated. Earlier, the gas was introduced at the top of the dewar. Several months of work were wasted trying to achieve reproducible results with this arrangement. Even with a 20 watt heater in the bottom of the dewar and the vigorous agitation by the gas entering the bottom of the liquid, an hour is needed for adequate mixing of 2 l of doped LAr. Once the dopant is well mixed in the LAr, there is no separation detected, even without further agitation.

There were three cells used in the dewar. The first contained an ^{241}Am alpha source at the center of a 2 mm gap, 25 mm in diameter. The electrode opposite the alpha source was

blackened with carbon to prevent reflection of the scintillation light not converted in the gap. This cell was used to measure the charge collected from a particle with a large dE/dx . The second cell was multi-layered and contained 720 cm² of 2 mm gaps, and containing no radioactive source. This was to search for breakdown or increased leakage current in the doped LAr. The third cell contained a 5×7.5 cm² depleted uranium plate as one electrode. This was used to search for instabilities in the doped LAr in a higher radiation environment.

To be brief, the second cell showed that there was no detectable increase in current in the doped LAr once it was properly mixed. The third cell showed that there was no breakdown problem in an uranium environment, at least at low concentrations of dopant. Therefore, all our results presented here will be taken from data with the alpha cell. It has also been shown that a LAr calorimeter, doped with allene, can be operated without problems[14].

Although there are over a dozen photosensitive dopants known to work with LAr, two have been shown to have significantly higher efficiencies[4]: allene (C₃H₄), and tetramethylgermanium (Ge(CH₃)₄), TMG. The allene was supplied by Matheson Gas Products and had a quoted minimum purity of 97%. The TMG used was manufactured by Wiley Organics and was 99.9% pure. The allene was purified by passing it through an Oxisorb cartridge. The TMG was vacuum distilled and stored on a baked out mixture of molecular sieve and silica gel.

The gas volume of the dewar and associated plumbing was carefully measured by releasing a known amount of gas into the evacuated system and monitoring the final pressure. The liquid volume of the system was measured and marked on the side of the dewar window in 200 cm³ intervals. Liquid levels between these marks were estimated by interpolation. The pressure in the dewar was measured with a mechanical manometer with an accuracy of 0.1 Torr at low pressures.

The desired initial dopant level was achieved by adding the dopant to the evacuated dewar to a predetermined pressure. The argon gas was then added and condensation begun. The dopant initially condensed on the cooling coils and was washed off by the condensing argon. Years of experience and careful measurements have convinced us that all of the dopant is devolved in the LAr by the end of the fill, particularly for the more soluble materials like allene and TMG. Subsequently lower concentration are achieved by draining out the appropriate amount of doped LAr and refilling the dewar.

4. Experimental Results

For the alpha-source cell, filled with pure LAr, a signal is only seen when the electrons are collected on the electrode opposite the source ("forward field"). This is because for the

detection of a pulse, the positive ions do not contribute on the time scale of the electronics. The contribution of an electron to the signal is proportional to the fraction of the gap width that it drifts[15]. Since the range of the alpha particle is only about 40 μm , when the electrons are collected at the alpha source (“reverse field”) they travel only a small distance and thus make an insignificant contribution. This is not so in the case of LAr containing a photosensitive dopant. Since the photon-absorption length of the photons, $\lambda(C)$, (which is a function of dopant concentration, C) can be on the order of the gap size, a signal is also seen for the reverse field case. Therefore, our pulse-height measurements were made as a function of dopant level and electric field strength for both forward and reverse fields. This gives additional information, since the reverse field signal is due solely to photoelectrons.

Figs. 2 and 3 show the normalized pulse heights as a function of dopant concentration for forward and reverse electric fields of 1.5 kV/mm for allene and TMG, respectively. For the forward field, as the concentration is decreased, $\lambda(C)$ increases. The average length that the photons travel before conversion increases and fewer photons convert within the gap. At $C=0$ (pure LAr) the pulse height is normalized to 1. At concentrations higher than reported on in this work, the pulse height for alpha particles is actually lower than for intermediate concentrations. This is due to enhanced recombination at the source (discussed below).

In the reverse field case, as the the concentration of dopant decreases, the average drift distance of the photoelectrons increases, but eventually fewer photons convert within the gap. The pulse height goes to zero as the concentration goes to zero.

Fig. 4 shows the normalized pulse height for forward and reverse fields of 2.5 kV/mm as a function of concentration for allene doped LAr. The effect of the dopant is lower than for 1.5 kV/mm. This is because at the higher electric field there is less recombination and therefore fewer photons produced.

Fitting the curves to the pulse-height spectra was quite complicated, and the details have been put as an appendix to this work. In the fitting process the forward and reverse field data were fitted at the same time, requiring a common photon conversion cross section for both curves. The quantum efficiency was taken to be 60% for both dopants. This value is consistent with the literature[16] and consistent with other fits that were made when the quantum efficiency was allowed to vary. We also assumed that efficiency of production of detectable photons was 0.79/recombination[17].

One consideration that was taken in the fitting process was that the presence of the dopant altered the amount of recombination from the alpha source. Since one is not able to measure the recombination for a photosensitive dopant, we measured the collected charge

for LAr doped with methane and ethane at the same levels. Both gases were quoted to be 99.99% pure.

Fig. 5 shows the relative pulse height as a function of concentration for methane doped LAr with an electric field of 1.5 kV/mm. The pulse height is normalized to 1 for $C=0$. There is a 20% drop in pulse height at $C = 10$ ppm. Ethane showed a slightly larger recombination than methane. We believe that the increase in recombination with increase in dopant level is due to the “cooling” of the excess electrons, shortening the thermalization distance, and thus increasing the recombination. It has always been assumed that photosensitive dopants are added at too low a level to affect the kinetic energy of the electrons. This has been shown to be a false assumption by Radeka’s group who have shown that 60 ppm of allene increases the electron drift velocity by about 50%[18]. In the fitting process, since we were not able to measure the recombination for the larger photosensitive molecules, the recombination was allowed to vary to give the best fit.

The fitted $\lambda(C)$ for a concentration of 10 ppm, λ_{10} , for the allene and TMG data are given in Table 1. The average values are 916 μm and 324 μm for allene and TMG, respectively. Although all the fits are very consistent, there are many uncertainties in the assumptions used to estimate the errors on λ_{10} . These values of λ_{10} yield cross sections of 44 Mb for allene and 154 Mb for TMG. It is reasonable that TMG has a much higher cross section than allene because of its size. Our determination of the photoelectric cross section of allene is a factor of two higher than has been measured by Suzuki[19].

As was stated above, the amount of recombination was allowed to vary in our fitting procedure. Figs. 6 and 7 show the direct charge (non-photoelectron component) taken from the fits. With the exception of the curve for 1 kV/mm, the allene data is similar to what was measured for methane. TMG shows a higher level of recombination, which is again consistent with its larger size.

5. Birk’s Constant

Having an estimate for alpha particles of the amount of direct ionization, number of photons, $\lambda(C)$, and, QE, one is in a position to calculate kB as a function for C for a given geometry. For dE/dx of the alpha particles, it was assumed that the 5.5 MeV was deposited uniformly along a 40 μm track. For dQ/dx of the alpha particle, the induced signal was calculated for an average position across the gap. (The exact details of the calculations can be found in the appendix.) Because the average position was used, the values of kB presented here are only correct for the average of many interaction as for a hadron shower in a calorimeter.

For our calculations of k_B , dQ/dx for a minimum ionizing particle was not measured. The value of dE/dx was taken from the literature to be $1.51 \text{ MeV g}^{-1} \text{ cm}^{-2}$ [20]. For the evaluation of eq. (1) we assumed that the shape of the curve of collected charge versus C was similar to that for the alpha particles, but with only a 10% increase at $C=10$. This assumption should give an error of dQ/dx of less than 5%, which is below other uncertainties in the calculation.

Figs. 8 and 9 show the estimated values of k_B as a function of dopant times gap size, $C \times d$ (ppm mm), and for different electric fields for allene and TMG, respectively. The effects of the larger cross section of TMG is apparent. One can see the dramatic effect in the value of k_B with the addition of as little as 2 ppm of either dopant to a LAr calorimeter with a gap as small as 2.5 mm. As was stated before, these values are only to aid in the calculation of the response of a calorimeter and not true for energy deposited in an arbitrary position in the gap.

6. Discussion

The measurement of e/π made by the NA34 collaboration and the Monte Carlo calculation made by J. Brau are compelling arguments that heavily ionizing interactions contribute to the signal in LAr hadron calorimeters, and that saturation effects play an important role in the e/π ratio. We estimate that the addition of 0.35% methane increases k_B by about a factor of 3.7, while the addition of a few ppm of TMG can reduce k_B by over a factor of 4. This would greatly improve the NA34 value of e/π . We have also confirmed the report[14] (at least for a small apparatus) that there seems to be no problem with the operation of a calorimeter with small quantities of well mixed dopants, even for high electric fields.

There are still two unanswered questions: breakdown of the dopants in a high rate environment, and the long decay constant of the scintillation light from LAr. The consideration of breakdown of the dopant is potentially more of a problem than one might first assume. Although the dopant would receive on the order of only 10^{-6} of the direct energy deposited in the LAr, there would be an ionized dopant molecule for every electron collected. The argon ions have a much higher affinity for an electron than the dopant molecules. Thus, in drifting across the gap each argon ion will do a charge exchange with a dopant molecule until all ions are dopant ions. This argues for making the initial tests of dopants at the few ppm level. At 2 ppm, even for the worse case of all the dopant dissociated into something as electronegative as oxygen, the calorimeter would still operate.

The concern that the long scintillation decay time of LAr will require a long electronic integration time in order to achieve the desired improvement of the e/π ratio. Table 2 lists

the decay times and fraction of the light in the short component of LAr for electrons and for alpha particles[21,22]. It can be seen from this table that for heavily ionizing interactions somewhere between 57% and 77% of the scintillation occurs in about 7 ns or less. The presence of the dopants may improve this even further by de-exciting the long lived states of the argon.

There is still work to be done on the possible problem of breakdown of the dopants at high rates, and on the time structure of the signal with the addition of these dopants. The next step will be to make a measurement of the change in the e/π ratio in a LAr calorimeter. We hope that this will be done in the near future.

7. Appendix - Details of Numerical Calculations

7.1 Forward Field Integral

The basic detector volume is shown in Figure 10. Consider photons emitted in the direction θ, ϕ with respect to the point at which the alpha particle deposits its energy. The photons convert at a distance r along this path with intensity

$$I(r) = \frac{I_0 \exp\left(-\frac{r}{\lambda}\right)}{\lambda r^2} \quad (2)$$

where I_0 is the photon intensity at the origin $\lambda(C)$ is the photon conversion length. The differential charge converted in the gap is

$$dq = \frac{QE N_\gamma}{4\pi} \frac{\exp\left(-\frac{r}{\lambda}\right)}{\lambda} \sin\theta \, dr \, d\theta \, d\phi \quad (3)$$

where N_γ is the total number of photons available for conversion (discussed in greater detail below) and QE is the quantum efficiency of the dopant.

The signal induced is proportional to the charge in the gap times the fraction of the gap each electron crosses. Thus eq. (3) must be weighted by a term:

$$\left(\frac{d-r\cos\theta}{d}\right). \quad (4)$$

where d is the gap size. The full integral for the forward field to be fitted, combining eqs. (3) and (4) and integrating over ϕ is:

$$Q_f(C) = \frac{QE N_\gamma}{4} \int_0^{\frac{\pi}{2}} \int_0^{\frac{d}{\cos\theta}} \frac{\exp\left(\frac{-r}{\lambda}\right)}{\lambda} \left(\frac{d-r\cos\theta}{d}\right) \sin\theta dr d\theta + N_e(C) . \quad (5)$$

Here $N_e(C)$ is the number of electrons that escape recombination and is a function of the electric field strength and (C) . For convenience $Q_f(0)$ has been normalized to equal 1. The integral of eq. (5) may be performed analytically to give,

$$Q_f(C) = \frac{QE N_\gamma}{4} \left(\left(\exp\left(\frac{-d}{\lambda}\right) \left(\frac{\lambda}{d} - 1 \right) + 2 - \frac{\lambda}{d} + \frac{d}{\lambda} E_i\left(\frac{-d}{\lambda}\right) \right) \right) + N_e(C), \quad (6)$$

where $E_i(x)$ is the exponential integral function.

An alpha particle deposits all of its energy in a very small volume, generating N_{ion} electron-ion pairs. The number of electrons which escape recombination, $N_e(C)$, will be a function of the electric field, E , and on C . At fixed E , N_γ is taken to be:

$$N_\gamma(C) = 0.79(N_{ion} - N_e(C)) , \quad (7)$$

where the factor of 0.79 represent the photon-quenching factor for alpha particles taken from the literature*. Because the addition of the photosensitive dopants “cool” the electrons, it effects their thermalization distance in the LAr. Since there is a relationship between the thermalization distance and the amount of recombination*, $N_e(C)$ will decrease with increasing C . For our fitting procedure, we have parameterized $N_e(C)$ as,

$$N_e(C) = N(0) \exp\left(\frac{-1}{k_1 + \frac{k_2}{C}}\right), \quad (8)$$

where k_1 and k_2 are constants determined by the fitting process. It can be seen by the fit of the methane data in fig. 5 that eq.(8) appears to be a suitable parameterization of $N_e(C)$.

7.2 Reverse Field Integral

For the reverse electric field, only the photoelectrons contribute to the induced charge. The integral describing the induced charge for the reverse electric field is:

$$Q_r(C) = \frac{QE N_\gamma}{4} \int_0^{\pi/2} \int_0^{\frac{d}{\cos\theta}} \frac{\exp(\frac{-r}{\lambda})}{\lambda} \left(\frac{r \cos\theta}{d} \right) \sin\theta dr d\theta . \quad (9)$$

Eq. (9) is identical to eq. (5) with the exception that there is no contribution from $N_e(C)$, and the term from eq. (4) becomes

$$\left(\frac{r \cos\theta}{d} \right), \quad (10)$$

reflecting the fact that the electrons drift the opposite direction. Eq. (9) can be solved, yielding:

$$Q_r(C) = \frac{QE N_\gamma}{4} \left(- \left(\exp(\frac{-d}{\lambda}) \left(\frac{\lambda}{d} + 1 \right) + \frac{\lambda}{d} + \frac{d}{\lambda} E_i(\frac{-d}{\lambda}) \right) \right). \quad (11)$$

7.3 Data Fitting

The data for the forward and reverse electric fields were simultaneously fit for a single value of $\lambda(C)$ at 10 ppm of dopant, λ_{10} . It was assumed that $\lambda(C)$ scaled inversely with C , i.e.,

$$\lambda(C) = \frac{10 \lambda_{10}}{C}. \quad (12)$$

Along with λ_{10} , k_1 , and k_2 were also allowed to vary in the fitting process. The fits to the data were quite good and described both the forward and reverse data well with a minimal number of assumptions. The $\chi^2/D.F.$ obtained for all fits were approximately 1.

7.4 Birk's Constant

In a LAr calorimeter, the heavily ionizing interactions will be evenly distributed throughout the gap. The charge collected in a short time from the direct charge is reduced by a factor of 2 since, on average, half the gap is traversed. The average induced charge for a heavily ionizing interaction is:

$$\langle Q_{HI}(C) \rangle = \frac{1}{2} N_e(C) + \langle Q_{pe} \rangle, \quad (13)$$

where $\langle Q_{pe} \rangle$ is the induced charge from the photoelectrons averaged across the gap. $\langle Q_{pe} \rangle$ is given by the integral:

$$\begin{aligned} \langle Q_{pe} \rangle = & \frac{QE N_\gamma}{2d} \int_0^d \int_0^{\frac{\pi}{2}} \int_0^{\frac{d-x}{\cos\theta}} \frac{\exp(\frac{-r}{\lambda})}{\lambda} \left(\frac{d-x-r\cos\theta}{d} \right) \sin\theta dr d\theta dx \\ & + \frac{QE N_\gamma}{2d} \int_0^d \int_0^{\frac{\pi}{2}} \int_0^{\frac{x}{\cos\theta}} \frac{\exp(\frac{-r}{\lambda})}{\lambda} \left(\frac{d-x+r\cos\theta}{d} \right) \sin\theta dr d\theta dx \end{aligned} \quad (14)$$

Where x is the coordinate of the interaction across the gap. This gives,

$$\langle Q_{pe} \rangle = \frac{QE N_\gamma}{4} \left(\left(\exp(\frac{-d}{\lambda}) \left(\frac{\lambda}{d} - 1 \right) + 2 - \frac{\lambda}{d} + \frac{d}{\lambda} E_i\left(\frac{-d}{\lambda}\right) \right) \right). \quad (15)$$

Eq. (1) relates dQ/dx to dE/dx through the parameter k_B and the constant of proportionality, c . The equation can be solved for k_B and c if the values of dQ/dx are provided for two values of dE/dx .

For the evaluation of eq. (1) the dE/dx for a minimum ionizing particle was used for a dE/dx of small value. For dQ/dx we assumed that the shape of the curve of collected charge verses C was similar to that for the alpha particles, but with only a 10% increase at $C=10$ over $C=0^*$. For heavily ionizing particles the dE/dx for an alpha particle was used and dQ/dx was obtained from $\langle Q_{HI}(C) \rangle$ by evaluating eqs. (13) and (14). As has been stated before, the results of these calculations contain uncertainties and are only intended to provide an estimate of the value of k_B for interactions averaged throughout the gap.

Table 1: Fitted $\lambda(C)$ for C=10 ppm for various electric fields.

Electric field (kV/mm)	Allene λ_{10} (μm)	TMG λ_{10} (μm)
1.0	932	322
1.5	921	324
2.0	902	326
2.5	909	325
	<916>	<324>

Table 2: Decay times for the fast τ_f and the slow τ_s components of the scintillation from LAr for electrons and alpha particles. The fraction of the scintillation in the fast component I_f is also given.

Particle	τ_f (ns)	τ_s (ns)	I_f (%)	Reference
Electron	4.6	1540	21	Carvalho and Klein ^a
	6 ± 2	1590 ± 100	23	Hitachi and Takahashi ^b
Alpha	4.4	1100	77	Carvalho and Klein ^a
	7.1 ± 1.0	1660 ± 100	57	Hitachi and Takahashi ^b

^aRef. 22

^bRef.21

Acknowledgements

The authors would like to thank Dr. K. Masuda from Saitama College and Dr. A. Hitachi from RIKEN for many useful discussions and guidance in understanding the literature on the subject.

References

- [1] S. Kubota, et al., Phys. Rev. B17 (1978) 2762.
- [2] T. Doke, et al., Nucl.Instr. and Meth. A235 (1985) 136.
- [3] D.F. Anderson, Nucl. Instr. and Meth. A242 (1986) 254.
- [4] D.F. Anderson, Nucl. Instr. and Meth. A245 (1986) 361.
- [5] S. Suzuki et al., Nucl. Instr. and Meth. A245 (1986) 78.
- [6] S. Suzuki et al., Nucl. Instr. and Meth. A245 (1986) 366.
- [7] K. Masuda et al., Nucl. Instr. and Meth. A245 (1986) 560.
- [8] H. Ichinose et al., Nucl. Instr. and Meth. A279 (1989) 354.
- [9] H. Gordon, et al., (The Calorimeter Team of the HELIOS Collaboration), Preliminary Performance Results of the HELIOS Uranium/Liquid Argon Hadron Calorimeter, CERN 077C, 1 August 1988.
- [10] J.E. Brau and K. Furuno, Hadron Calorimetry - Optimizing Performance, preceedings of the Internation Conference on Calorimetry in High Energy Physics, Fermilab, Oct. 29- Nov. 1.
- [11] D.F. Anderson and D.C. Lamb, Nucl. Instr. and Meth. A265 (1988) 440.
- [12] E. Shibamura et al. Nucl. Instr. and Meth. 131 (1975) 249.
- [13] H. Volk and G.D. Halsey, Jr., J. Chem. Phys. 33 (1960) 1132.
- [14] T. Doke et al., Liquid Argon Calorimeter Doped with Allene for High Energy Heavy Ions, Report of Sci. and Eng. Res. Lab., Waseda University NO.90-12, 29 Oct, 1990, Submitted to Nucl. Instr. and Meth.
- [15] W.J. Willis and V. Radeka, Nucl. Instr. and Meth. 120 (1974) 221.
- [16] K. Masuda et al. Nucl. Instr. and Meth. A279 (1989) 560.
- [17] A. Hitachi, A. Yunoki, and T. Doke, Phys. Rev. A 35 (1987) 35.
- [18] V. Radeka, private communications.
- [19] S. Suzuki, Thesis, Waseda Univ. (1986) (in Japanese).
- [20] Particle Data Group, "Review of Particle Properties," Phys. Lett. B239, April 1990.
- [21] A. Hitachi and T. Takahashi, Phys. Rev. B 27 (1983) 5279.
- [22] M.J. Carvalho and G. Klein, J. Lumin. 18-19 (1979) 487.

Figure Captions

Figure 1: NA34 measurement of e/π as a function of beam energy measured with pure LAr and LAr doped with 0.35% methane[9]. The fit to these data has been added to guide the eye.

Figure 2 : Normalized pulse height as a function of allene concentration for both forward and reverse electric fields of 1.5 kV/mm.

Figure 3 : Normalized pulse height as a function of TMG concentration for both forward and reverse electric fields of 1.5 kV/mm.

Figure 4 : Normalized pulse height as a function of allene concentration for both forward and reverse electric fields of 2.5 kV/mm.

Figure 5 : Relative pulse height as a function of methane concentration for an electric field of 1.5 kV/mm.

Figure 6 : Direct charge as a function of allene concentration taken from the fits, for various electric field strengths.

Figure 7 : Direct charge as a function of TMG concentration taken from the fits, for various electric field strengths.

Figure 8 : Birk's constant as a function of the product of allene concentration times gap size for various electric field strengths.

Figure 9 : Birk's constant as a function of the product of TMG concentration times gap size for various electric field strengths.

Figure 10: Coordinate system used for the calculations.

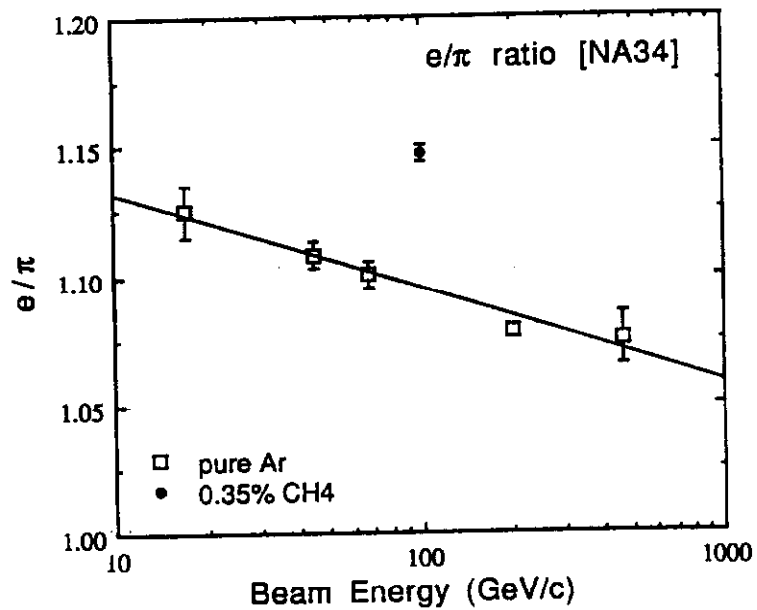


Figure 1

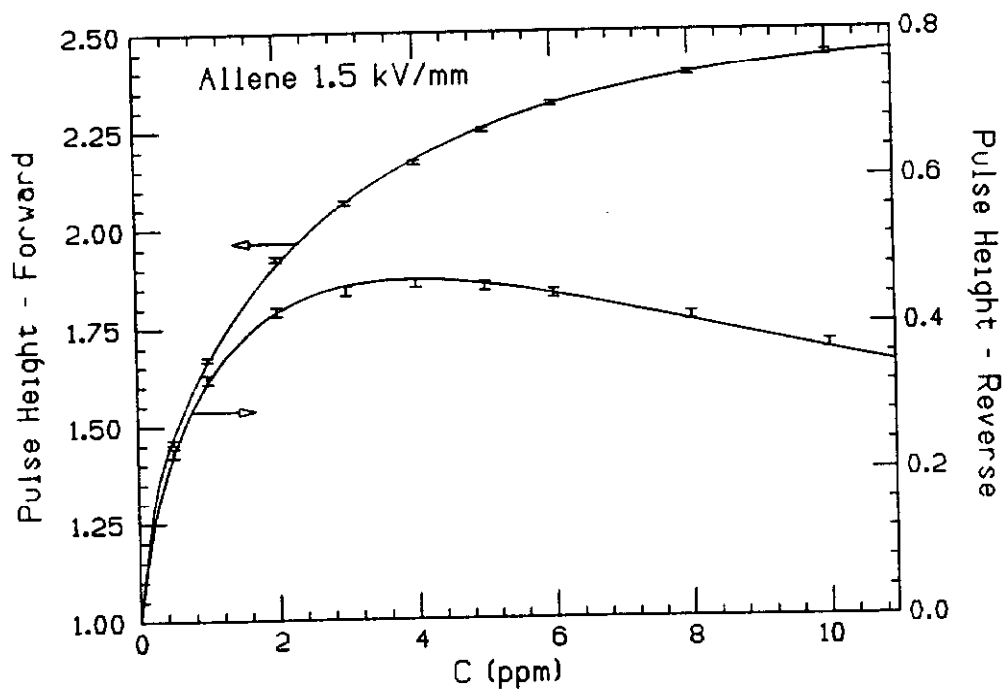


Figure 2

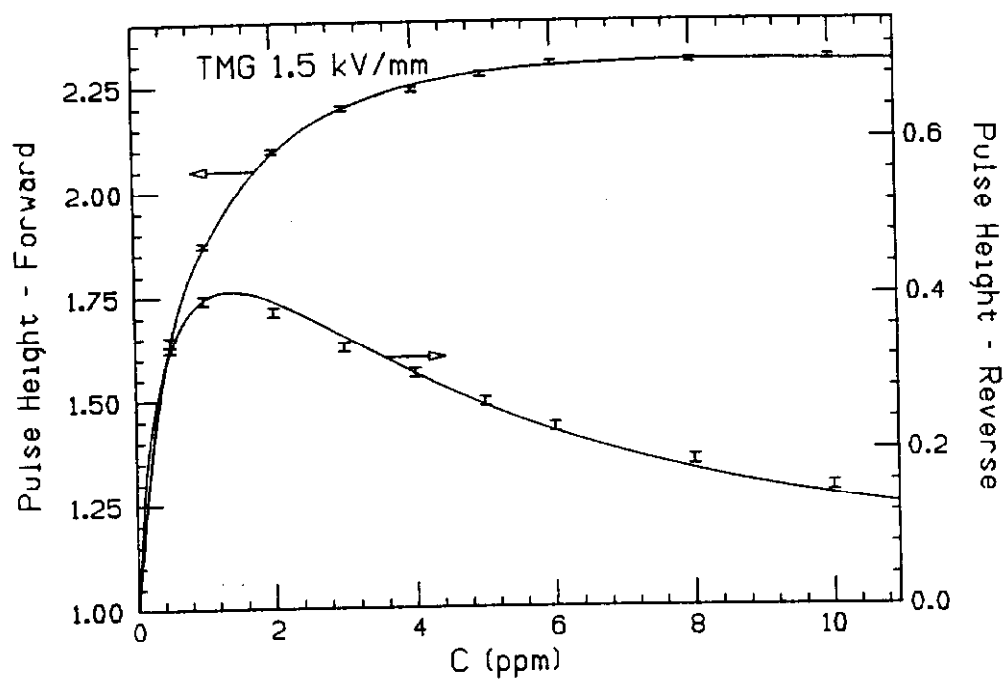


Figure 3

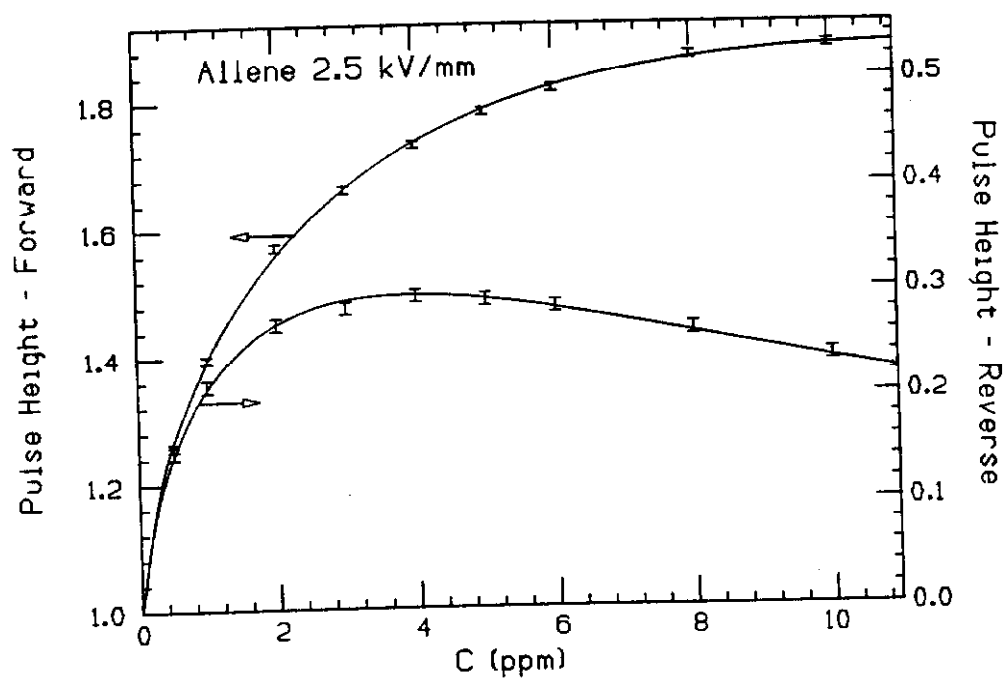


Figure 4

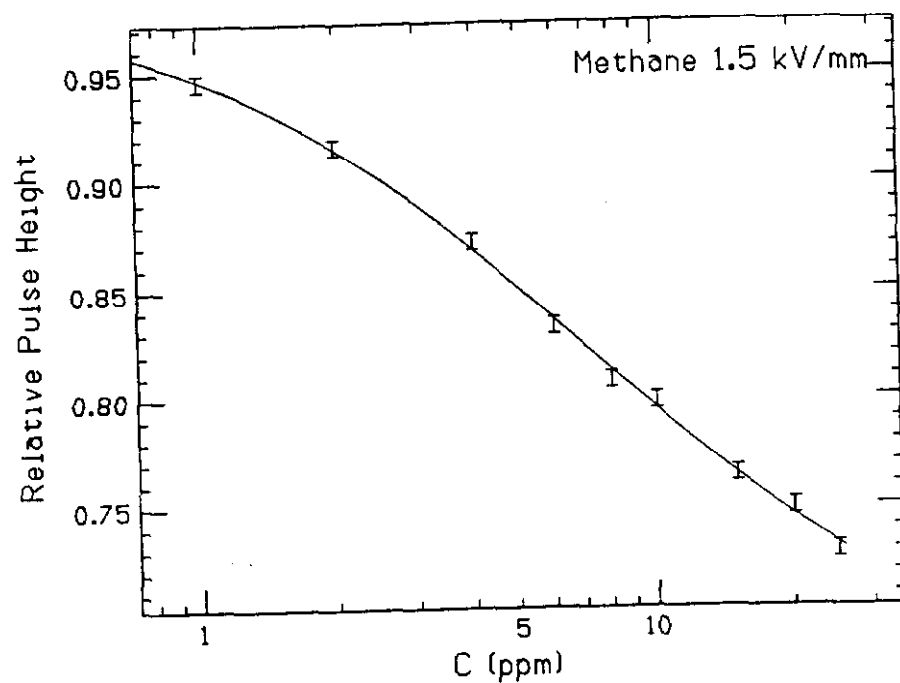


Figure 5

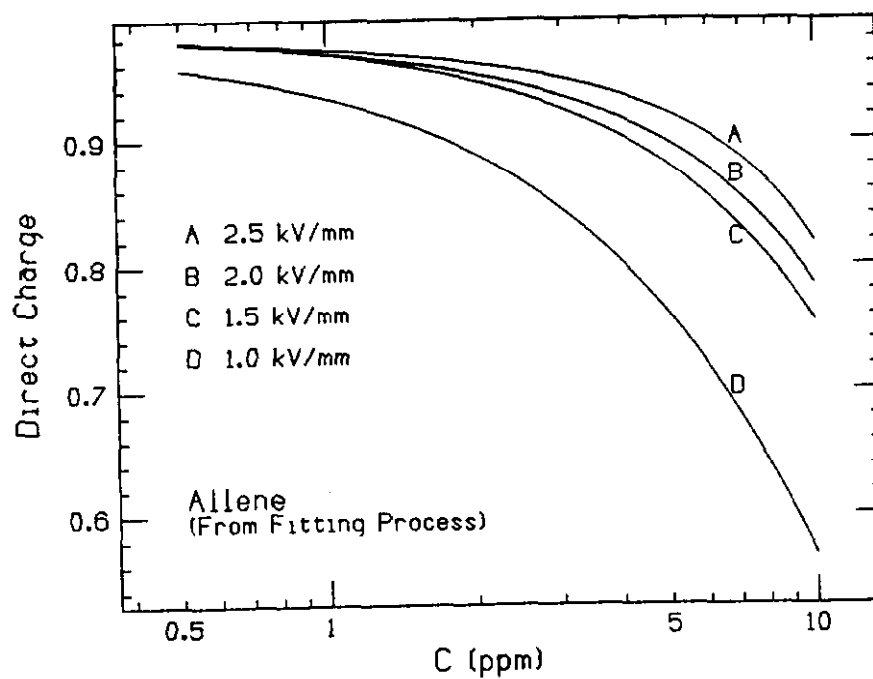


Figure 6

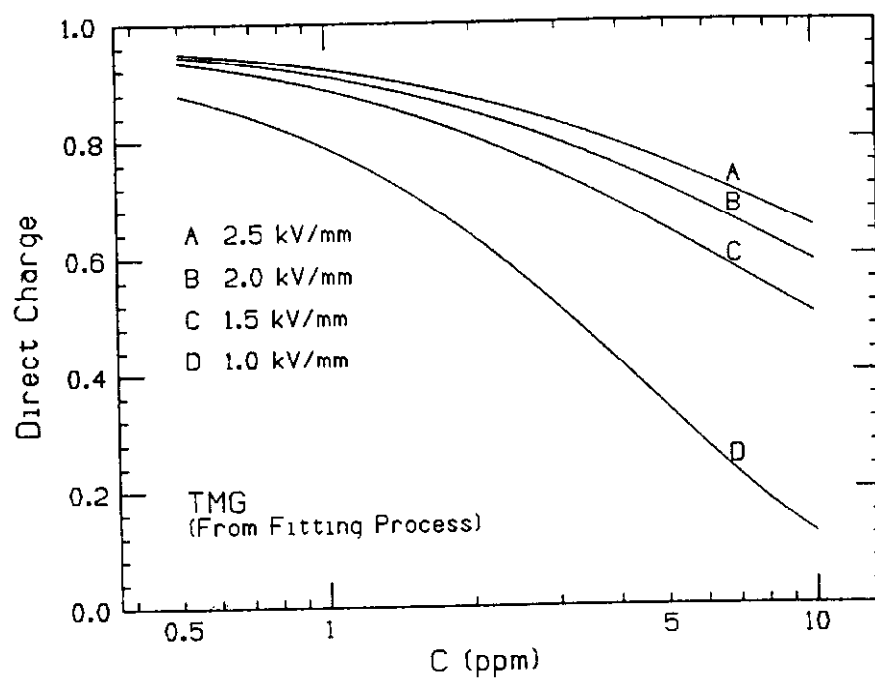


Figure 7

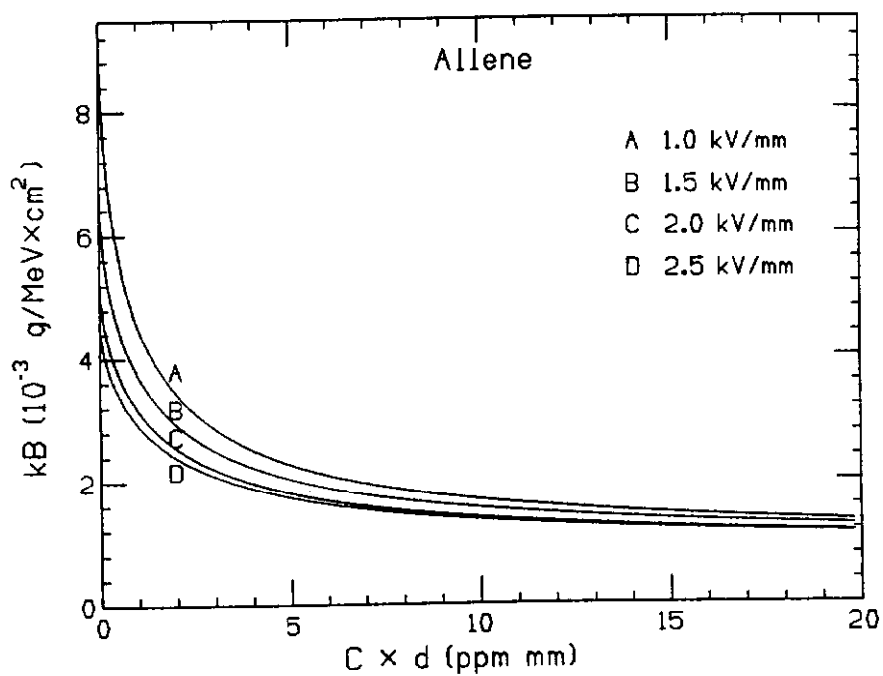


Figure 8

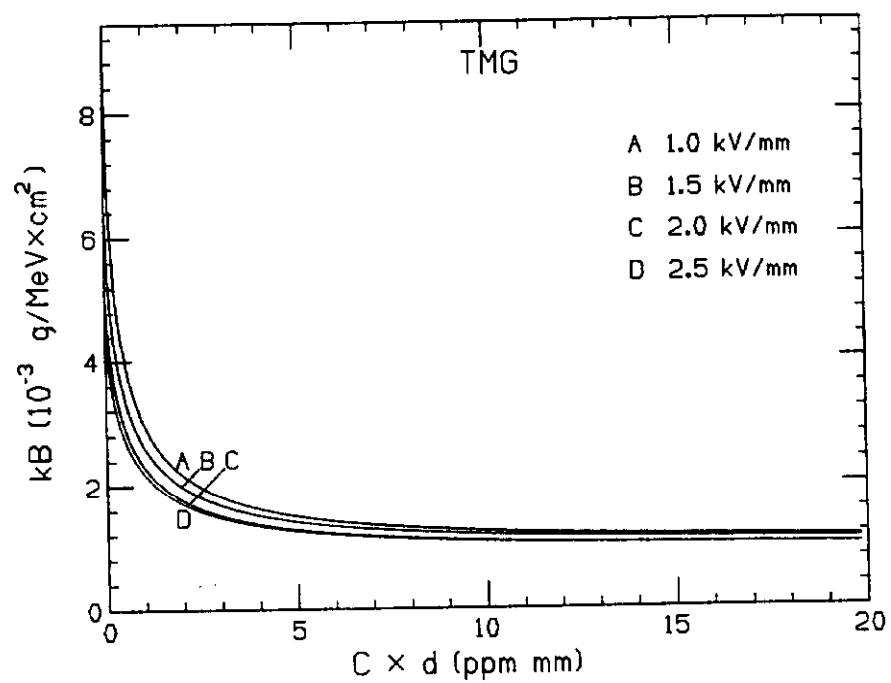


Figure 9

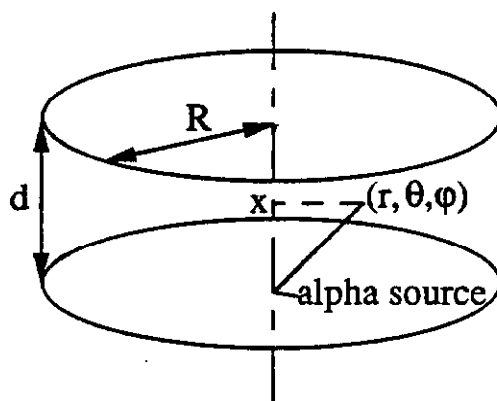


Figure 10